Design of a Multi-layered On-chip Wireless Power Transfer (WPT) System Design for Brain Neuromodulation Applications

Dipon K. Biswas, Bernabe Rangel, and Ifana Mahbub
Department of Electrical Engineering, University of North Texas, Denton TX 76207, USA

***Abstract*—Chronic pain is a common disease and as a negative consequence can cause paralysis to an individual in the long run. Noninvasive brain stimulation is an effective method to reduce pain in the short term. However, for long-term treatment, neural data analysis along with the stimulation is highly desirable. In this work, a unique multilayer spiral coil with a total dimension of 500 μm × 500 μm is designed in a 0.5 μm CMOS process to make it suitable for a fully implantable system. The electrical modeling of the coil is also analyzed and simulated using Keysight's Advanced Design System (ADS) software to compare the theoretical modeling results with the simulation results. The electromagnetic (EM) simulation to characterize the on-chip coil in-terms of scattering parameters (S-parameters), Q-factor, power transfer efficiency (PTE) is performed using the Ansys High-Frequency Structure Simulator (HFSS) software. The operating frequency of the WPT system is chosen to be within 402-405 MHz which is the Medical Implant Communication System (MICS) band. The simulated Q-factor of the proposed on-chip coil is approximately 15 at 402 MHz. The on-chip coil is integrated with an on-chip seven-stage rectifier and some commercial off-the-shelf (COTS) components such as a DC-DC converter and a µLED to design the complete optogenetic neuro-stimulation system. A minimum power transfer efficiency (PTE) of 0.4% is achieved through a 16 mm thick tissue media using the proposed WPT system. With that efficiency, the proposed system is able to provide constant power to light up a µLED and proves to be a good candidate for neuromodulation applications.**

***Index Terms*—Neuromodulation application, Wireless power transfer, CMOS, Implants, on-chip, Q-factor.**

I. Introduction

The development of implantable medical devices has become a priority due to the high demand for advanced medical treatment for diseases like cardiac arrest, hearing disability, blindness, Parkinson's disease, and epilepsy [1]–[4]. Modern implantable system mainly focuses on accomplishing a low form-factor, low-cost, lightweight, reliability and a longer lifetime [5]. One of the major uses of an implantable medical device is for the treatment of Parkinson's disease which requires a deep brain stimulation and recording system [6]. Such an implantable system requires a better and efficient power source than a battery for which a patient needs to go through multiple surgeries for the replacement of the battery. The frequent surgeries can cause inconvenience and pose safety concerns to the patient's health. Thus, a wireless power transfer (WPT) method based on inductive coupling can provide a better solution to this problem which eliminates the requirement for surgeries. Furthermore, to reduce the size and weight of the implant, an integrated on-chip-based neural stimulation circuit can be the best choice. Prior works have demonstrated the design of the inductor coil for the receiver (RX) WPT system being designed using complementary metal-oxide-semiconductor (CMOS) process [7]–[9]. However, most of the designs operate in the GHz frequency range and none of them are used for biomedical applications.

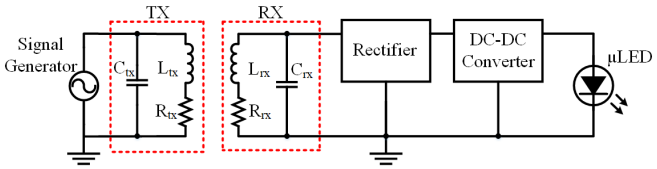

Fig. 1: Wireless power transfer based neural stimulation system.

In this work, an on-chip based novel spiral multilayer receiver (RX) coil designed to operate in the MICS band is proposed along with an on-chip rectifier circuit to provide DC power. A DC-DC converter is also integrated with the on-chip coil and rectifier to provide constant power to the stimulator module which includes a mini or μLED for the case of optogenetic application. Depending on the brain region that requires stimulation and the particular neuromodulation application, the stimulator module might require a constant intensity level. The proposed on-chip WPT system designed in 0.5 μm CMOS process is integrated with a commercially available DC-DC converter to provide a constant voltage to the LED for optogenetic neuromodulation application.

The main contribution of this work is the design of a complete and efficient WPT system to provide constant power for neural stimulation. The paper is organized as follows: section II presents an overview of the system including the transmitter (TX) and the RX coils, rectifier and the DC-DC converter circuits; section III presents the simulation results demonstrating the validation of the proposed system, followed by concluding remarks presented in section IV.

II. System Overview

In an optogenetic neural stimulation, a light source such as Light amplification by stimulated emission of radiation (LASER) or Light emitting diode (LED) is used to stimulate the genetically modified neurons. A simplified block diagram of the proposed WPT based optogenetic neural stimulation system is shown in Fig. 1. The typical WPT system follows

978-1-7281-1803-1/19/$31.00 ©2020 IEEE

TABLE I
Proposed Coil Dimensions

Parameters	RX coil	TX coil
Diameter	500 μM	20 mm
Number of turns	M_1 layer: 2 M_2 layer: 1.5	2
Trace width	50 μm	1 mm
Trace spacing	50 μm	1 mm

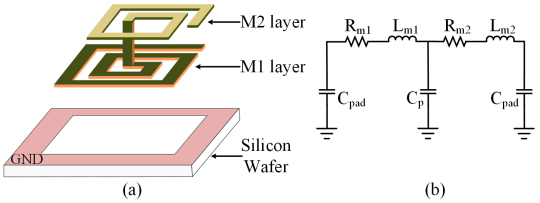

Fig. 2: (a) Exploded view of the on-chip multilayer coil, and (b) equivalent model of the multilayer coil.

the inductive-coupling method of transferring power using a TX-RX pair. The TX and RX coils are represented with the inductance, L_{tx} and L_{rx}, respectively and the R_{tx} and R_{rx} represent the series resistances associated with the coils. C_{tx} and C_{rx} are the two resonating capacitances which are used to resonate the TX and RX coils respectively to the desired operating frequency range. The received AC power coming from the TX is rectified using a rectifier to provide a DC voltage at the load. As the neural stimulator requires a constant power irrespective of the distance variations between the TX and RX coils, a DC-DC converter is used in this work to provide a constant DC voltage and current to the μLED that is used as a load in this work.

A. RX Coil Design

The proposed RX coil is a multilayer square spiral coil designed in 0.5 μm CMOS process. As shown in Fig 2(a), the RX spiral coil is designed using metal layer, M_1 and M_2 over a silicon wafer. The total dimension of the on-chip coil is 500 μm $\times$ 500 μm. The M_1 layer is used to design a square spiral with 2 turns having the trace width and trace spacing of 50 μm as listed in Table I. To minimize the capacitance of the stacked metal layers, the top spiral is designed using M_2 layer over the spacing of the bottom spiral coil. The top and the bottom layers are separated by a silicon-dioxide (SiO_2) layer. A metal interconnect (via) is used to connect the top and the bottom layers. The electrical modeling of the on-chip coil is shown in Fig 2(b). L_{m1} and R_{m1} denote the inductance and the resistance, respectively for the M_1 layer. For the M_2 layer, the inductance is denoted by L_{m2} and the associated series resistance by R_{m2}. The capacitance between the two metal layers are represented by C_p and C_{pad} denotes the capacitance due to the bond pad.

The inductor of the top and the bottom metal layers can be calculated using equation (1) where K_1 and K_2 are constants and for the square spiral, the values are 2.34 and 2.75, respectively. N is the number of turns and μ_0 is the permeability of the free space.

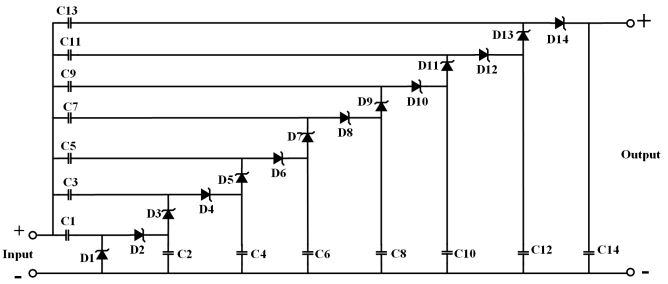

Fig. 3: Schottky diode based seven-stage rectifier.

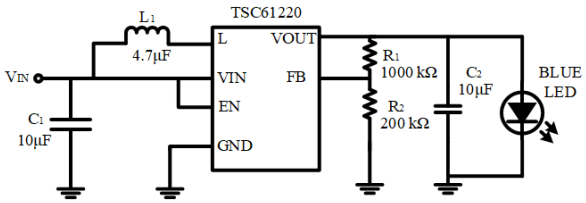

Fig. 4: Functional block diagram of the TPS61220 boost converter.

$$L = \frac{K_1 \mu_0 N^2 d_{avg}}{1 + \phi K_2} \tag{1}$$

The average diameter, d_{avg} is the average of the outer diameter, D_o and the inner diameter, D_i of the coil as shown in equation (2).

$$d_{avg} = \frac{D_o + D_i}{2} \tag{2}$$

$$Fill\,ratio, \phi = \frac{D_o - D_i}{D_o + D_i} \tag{3}$$

B. Rectifier

The proposed rectifier circuit is a Schottky diode-based seven-stage rectifier circuit designed on-chip as shown in Fig. 3. The Schottky diode is used due to its low forward voltage requirement. A single-stage of the rectifier consists of two Schottky diodes, $D1$ and $D2$, an input capacitor, $C1$, and an output capacitor, $C2$ through which the output is fed to the next stage of the rectifier [10]. For every stage in the design, the input and the output capacitors are chosen to be 10 pF and 100 pF, respectively. The seven-stage architecture for the rectifier is chosen to have an output voltage of seven times that of the input voltage. The layout of the on-chip based rectifier takes up to 700 μm $\times$ 600 μm area of the chip.

C. DC-DC converter

A commercially available off-the-shelf component, TPS61220 by Texas Instruments is used as the DC-DC converter for this work. As shown in Fig. 4. The TPS61220 boost converter receives varying input DC voltages from the rectifier and outputs a constant DC voltage concurrent to the external resistor divider (R_1 and R_2). The input capacitor (C_1) helps eliminate the fluctuations in the input voltage of the regulator to assist with the transient behavior. The

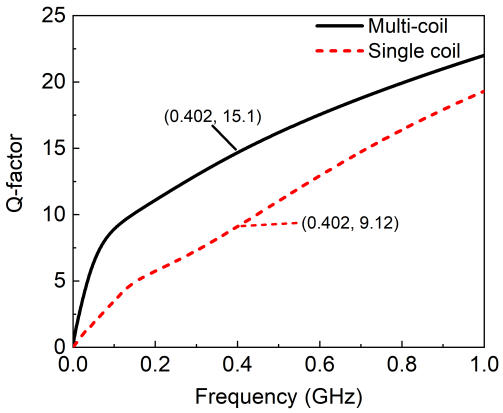

Fig. 5: Simulated Q-factor of the proposed on-chip multi-layer RX coil and conventional single layer coil.

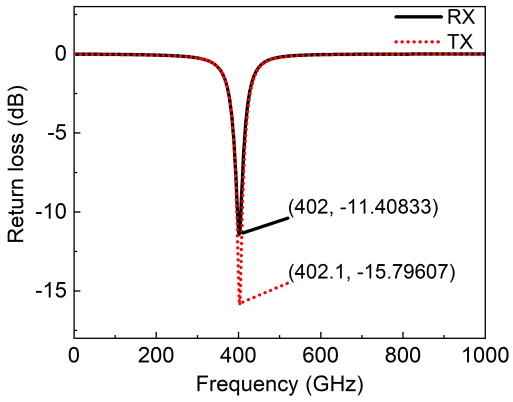

Fig. 6: Simulated return loss of the RX and TX coils.

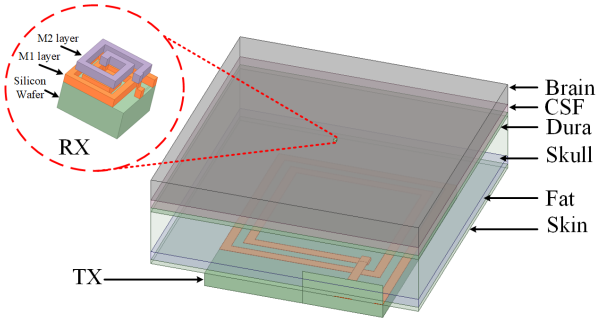

Fig. 7: Simulation setup in HFSS showing the TX and RX coils along with the six-layer brain tissue model.

output voltage, V_{out} is regulated using a hysteric-mode by keeping the inductor's current (L_1) constant at 200 mA. A feedback loop and an external reference voltage source are connected to a voltage error amplifier to drive the inductor current higher by increasing the voltage across the inductor. During the steady-state operation, the inductor's current charges the output capacitor (C_2) and flows into the LED. When the output voltage reaches equilibrium the load LED is powered through the output capacitor that is being charged and discharged by a couple of internal power MOSFETs.

The luminous intensity of the LED model XZCM2CRK53WA-8VF by SunLED is current dependent, i.e. for a relative luminous intensity of 1, a 2 mA current source is required. The LED has a minimum forward voltage requirement of 1.8 V. Thus, a maximum voltage output of 3 V is selected for the TPS61220 (DC-DC converter) resulting in an output current of 9 mA. The minimum voltage required to activate the TPS61220 chip is 0.7 V. For an input voltage range of 0.7 V to 5.5 V, the output voltage V_{out} is regulated to 3 V using a simple voltage divider where a 1 MΩ resistor is placed at R_1 and 200 kΩ resistor is placed at R_2, as shown in Fig. 4. The voltage divider's output serves as the reference voltage that feeds into the internal feedback loop to set the output voltage.

D. TX Coil Design

A 20 mm × 20 mm square shaped TX coil is proposed for the characterization of the PTE of the proposed WPT system [11]. The copper conductor-based TX coil is a 2-turn square spiral designed on FR4 substrate. The trace width and the spacing of the TX is coil is set to be 1 mm.

III. Resutls and Discussion

The on-chip multilayer spiral coil is modeled using Ansys HFSS software to characterize the return loss, Q-factor and the PTE. The operating frequency is chosen to be 402 MHz which is within the MICS band (402-405 MHz). The simulated Q-factor at 402 MHz frequency is ∼15 for the RX multi-coil as shown in Fig. 5. The Q-factor of the proposed multilayer coil is higher than the conventional single-layer on-chip coil (Q-factor value of 9 as shown in Fig. 5) as the inductance is increased by adding an additional spiral conductor layer on top of the bottom layer. To resonate the RX coil at 402 MHz, a resonating capacitor of 147 pF is used. The return loss of the RX coil presented in Fig. 6 (solid line) shows the value of -11.4 dB at 402 MHz frequency. The return loss of the TX coil is also simulated using HFSS. The TX coil is designed in such a way that with a resonating capacitor of 3.2 pF, the TX coil resonates at 402 MHz frequency. The return loss of the TX coil is also shown in Fig. 6 (dotted line) which shows the maximum return loss of -15.79 dB at 402 MHz frequency.

As the proposed system is designed to be used as an implantable system, the PTE simulation for the system is analyzed through the brain tissue media. A six-layer brain tissue model consisting of skin, fat, skull, dura, CSF and brain is designed using HFSS as shown in Fig. 7 [11]. The different tissue layers consist of different dielectric properties which are incorporated in the HFSS model to emulate the heterogeneous behavior of the brain tissue model [12]. The values of the conductivity and relative permitivity of the various brain tissue layers used in HFSS are tabulated in Table II. To determine the maximum allowable transmitted power for this system through the tissue media, an SAR simulation is performed. Fig. 8 shows that the system can transmit a maximum of 19 dBm power for which the SAR value is 1.58 W/kg. According to the Federal Communication Commission (FCC) regulation,

TABLE II
Tissue properties
for different brain tissue layers

Layers	Relative Permittivity, ϵ	Conductivity, σ (S/m)	Thickness (mm)
Skin	46.7	0.69	1
Fat	5.6	0.04	2
Skull	17.8	0.16	7
Dura	46.7	0.83	1
CSF	71	2.25	2
Brain	49.7	0.59	40

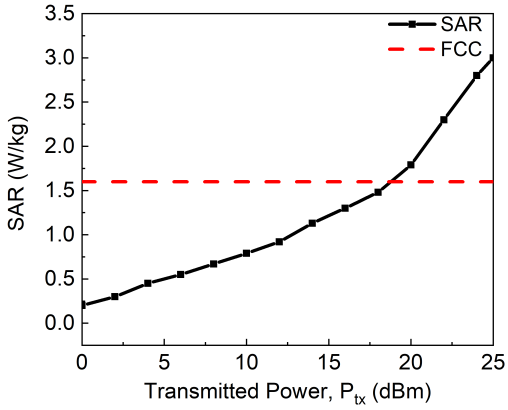

Fig. 8: Simulated SAR vs. Transmitted power.

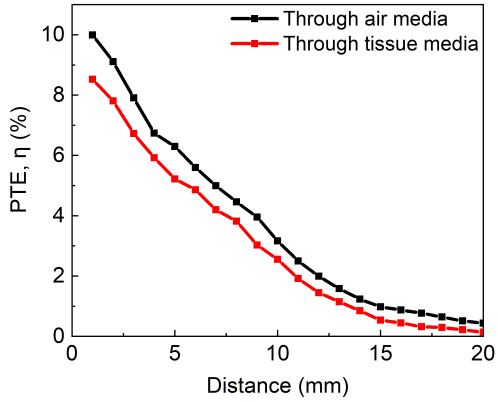

Fig. 9: Simulated PTE through air media and tissue media over various distances.

1.6 W/kg is the maximum allowable SAR value [13].

The PTE of the system is simulated for different distances ranging from 1 to 20 mm. The PTE, η is calculated based on the transmitted power, P_{tx} and the received power, P_{rx} as mentioned in equation (4).

$$\eta = \frac{P_{rx}}{P_{tx}} \times 100\% \tag{4}$$

As shown in Fig. 9, the maximum PTE value is $\sim$ 8.5% at 1 mm distance and the minimum PTE is 0.2% at 20 mm distance

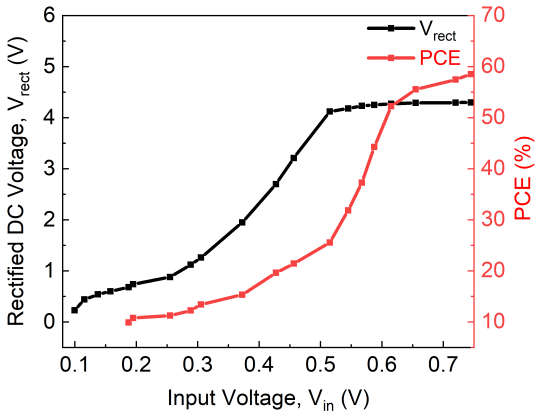

Fig. 10: Rectified DC voltage output and PCE over different input voltages.

through the tissue media. With the increase in the distance, the PTE decreases for a fixed transmitted power. In this work, the transmitted power is set to be 19 dBm and the TX and RX coils are considered to be perfectly aligned. The misalignment study between the TX-RX coils have been studied in our prior work and thus has not been included in this work [14]. With the 19 dBm transmitted power, the minimum AC voltage received by the RX coil is 0.1 V_p at 20 mm distance through the tissue media. As the proposed rectifier has a minimum input voltage requirement of 0.17 V_p, the rectifier will not be able to work when the TX-RX pair is 20 mm apart. The rectified DC output voltage of the rectifier varies with the varying input voltage. At the minimum input voltage of 0.18 V_p which is received through 16 mm of tissue layer, the rectified DC voltage, V_{rect} is reported as 0.68 V DC as shown in Fig. 10. The rectified DC voltage can be as high as 4.3 V with an input voltage of 0.7 V when the distance between the TX and RX coils is 1 mm. Due to the forward voltage drop of Schottky diodes, the output of the seven stage rectifier is lower than the expected seven times of the input voltage. The PCE of the rectifier at 1 mm distance between the TX and the RX coils is calculated to be 58% according to equation (5) which is also shown in Fig. 10.

$$PCE = \frac{\frac{V_{rect}}{R_{out}}}{\frac{V_{in}}{R_{in}}} \times 100\% \tag{5}$$

where R_{out} is the load resistance of the rectifier and R_{in} is the input impedance of the rectifier. The input impedance of the rectifier is found to be approximately 1 kΩ from the simulation and a 10 kΩ resistance is used as load resistance.

The commercially available DC-DC converter model is simulated using PSpice software. As mentioned in section II, the voltage range of the TPS61220 boost converter is 0.7 to 5.5 V, which requires the minimum DC voltage output from the rectifier to be 0.7 V which is achieved with 0.2 V_p input voltage at the rectifier and the distance between the TX-RX pair for that case is 14 mm. The simulated voltage output of the boost converter is shown in Fig. 11. It can be seen from the figure that the output voltage of the boost

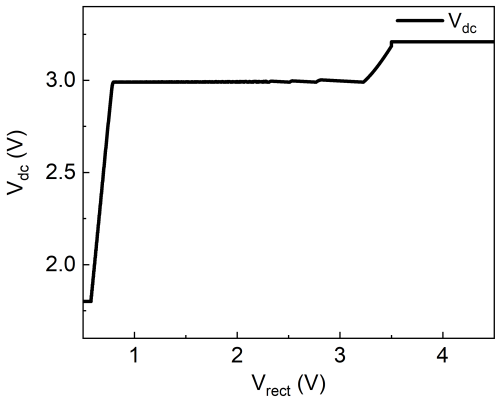

Fig. 11: Output voltage of the TPS61220 boost converter with respect to the input voltage coming from the rectifier output.

converter, V_{dc} is constant 3 V when the V_{rect} is within 0.7 V to 3.3 V. Above 3.3 V, V_{dc} shows a slight increase in the output voltage showing a value of 3.2 V. A μLED (XZCM2CRK53WA-8VF by SunLED) with a minimum 1.8 V forward voltage and 2 mA forward current is used as the load in the proposed neuromodulation circuit. The proposed system is able to provide a constant voltage of 3 V to the μLED which produces a constant intensity to stimulate the target neurons.

IV. Conclusion

A complete, miniaturized WPT system is proposed for an implantable neural stimulation device that is able to provide a constant voltage to the μLED irrespective of the distance of operation ranging from 1 to 16 mm. The proposed on-chip multilayer RX coil is designed in such a way that it has a minimum parasitic capacitance thus achieving a high Q-factor. The integration of an on-chip DC-DC converter rather than using a commercially available component can make the whole system further miniaturized which is a future work of this research. The future work also includes the design of the neural signal recording and wireless data transmission circuit which will enable the continuous wireless neural stimulation and recording system for the next-generation of neuromodulation and other neural interfacing applications.

Acknowledgment

This material is based upon work supported by the National Science Foundation under Grant No. ECCS 1943990.

References

[1] K.-J. Chen, W.-M. Chen, L.-Y. Tang, Y.-T. Cheng, M.-D. Ker, and C.-Y. Wu, "A 13.56 mhz metamaterial for the wireless power transmission enhancement in implantable biomedical devices," in *2019 20th International Conference on Solid-State Sensors, Actuators and Microsystems & Eurosensors XXXIII (TRANSDUCERS & EUROSENSORS XXXIII)*. IEEE, 2019, pp. 1439–1442.

[2] L. S. Wong, S. Hossain, A. Ta, J. Edvinsson, D. H. Rivas, and H. Naas, "A very low-power cmos mixed-signal ic for implantable pacemaker applications," *IEEE Journal of solid-state circuits*, vol. 39, no. 12, pp. 2446–2456, 2004.

[3] G. Wang, W. Liu, M. Sivaprakasam, and G. A. Kendir, "Design and analysis of an adaptive transcutaneous power telemetry for biomedical implants," *IEEE Transactions on Circuits and Systems I: Regular Papers*, vol. 52, no. 10, pp. 2109–2117, 2005.

[4] W. Liu, M. Sivaprakasam, G. Wang, M. Zhou, J. Granacki, J. LaCoss, and J. Wills, "Implantable biomimetic microelectronic systems design," *IEEE engineering in medicine and biology magazine*, vol. 24, no. 5, pp. 66–74, 2005.

[5] R. Erich, "Trends in microelectronic assembly for implantable medical devices," in *2007 32nd IEEE/CPMT International Electronic Manufacturing Technology Symposium*. IEEE, 2007, pp. 103–107.

[6] M. Sommer, E. M. Stiksrud, K. von Eckardstein, V. Rohde, and W. Paulus, "When battery exhaustion lets the lame walk: a case report on the importance of long-term stimulator monitoring in deep brain stimulation," *BMC neurology*, vol. 15, no. 1, p. 113, 2015.

[7] G. Lihui, Y. Mingbin, C. Zhen, H. Han, and Z. Yi, "High q multilayer spiral inductor on silicon chip for 5/spl sim/6 ghz," *IEEE Electron device letters*, vol. 23, no. 8, pp. 470–472, 2002.

[8] M. Raieszadeh, P. Monajemi, S.-W. Yoon, J. Laskar, and F. Ayazi, "High-q integrated inductors on trenched silicon islands," in *18th IEEE International Conference on Micro Electro Mechanical Systems, 2005. MEMS 2005.* IEEE, 2005, pp. 199–202.

[9] T. Kaho, M. Sasaki, Y. Yamaguchi, K. Nishikawa, and K. Uehara, "Miniaturized multilayer inductors on gaas three-dimensional mmic," in *2007 Korea-Japan Microwave Conference*. IEEE, 2007, pp. 149–152.

[10] N. T. Tasneem, S. R. Suri, and I. Mahbub, "A low-power cmos voltage boosting rectifier for wireless power transfer applications," in *2018 Texas Symposium on Wireless and Microwave Circuits and Systems (WMCS)*. IEEE, 2018, pp. 1–4.

[11] M. Sinclair, D. Biswas, T. Le, J. Hyde, I. Mahbub, L. Chang, and Y. Hao, "Design of a flexible receiver module for implantable wireless power transfer (wpt) applications," in *2019 United States National Committee of URSI National Radio Science Meeting (USNC-URSI NRSM)*. IEEE, 2019, pp. 1–2.

[12] J. Kim and Y. Rahmat-Samii, "Implanted antennas inside a human body: Simulations, designs, and characterizations," *IEEE Transactions on microwave theory and techniques*, vol. 52, no. 8, pp. 1934–1943, 2004.

[13] J. C. Lin, "A new IEEE standard for safety levels with respect to human exposure to radio-frequency radiation," *IEEE Antennas and Propagation Magazine*, vol. 48, no. 1, pp. 157–159, 2006.

[14] D. K. Biswas, N. T. Tasneem, and I. Mahbub, "Effects of coaxial-lateral and coaxial-angular displacements on link efficiency of a wirelessly powered optogenetic implant: Design, modeling, and experimental validation," *IEEE Journal of Electromagnetics, RF and Microwaves in Medicine and Biology*, vol. 3, no. 4, pp. 269–275, 2019.